

Helmut Hachul, Daniela Ridder-Weßels, Yesim Tekinbas
Fachhochschule Dortmund, Fachbereich Architektur

Thorsten Weimar, Henrik Reißaus
Universität Siegen, Lehrstuhl für Tragkonstruktion

Entwicklung ressourcenschonender und materialeffizienter Unterkonstruktionen aus feuerverzinktem Stahl für vorgehängte hinterlüftete Fassaden

Bericht Nr. 175
Gemeinschaftsausschuss Verzinken e.V.
2023



Gefördert durch:



Bundesministerium
für Wirtschaft
und Klimaschutz

aufgrund eines Beschlusses
des Deutschen Bundestages

Dieser Bericht stellt die Ergebnisse eines Forschungsprojektes der AiF-Forschungsvereinigung GAV dar. Die Untersuchungen wurden vom Bundesministerium für Wirtschaft und Klimaschutz über die Arbeitsgemeinschaft industrieller Forschungsvereinigungen e.V. (AiF) gefördert; AiF-Forschungsvorhaben IGF 21061 N.

Entwicklung ressourcenschonender und materialeffizienter Unterkonstruktionen aus feuerverzinktem Stahl für vorgehängte hinterlüftete Fassaden

Development of resource-saving and material-efficient substructures made of bath galvanized steel for rear ventilated facades

**M.Sc. Henrik Reißaus¹, Univ.-Prof. Dr.-Ing. Thorsten Weimar¹
Daniela Ridder-Weßels M.Sc.², Yesim Tekinbas M.Sc.², Prof. Dr.-Ing. Helmut Hachul²**

¹ *Universität Siegen, Institute of Structural Design, Hölderlinstraße 3, 57068 Siegen
E-Mail: reissaus@architektur.uni-siegen.de*

² *Dortmund University of Applied Sciences and Arts, Department Architecture, Teaching and research area
architecture and metal construction, Emil-Figge-Straße 40, 44277 Dortmund
E-Mail: helmut.hachul@fh-dortmund.de*

Summary

The article describes the material-efficient development of brackets made of bath galvanized steel for the rear-ventilated façades. The focus of the investigations is on the reduction of thermal bridges with analogous high mechanical strength.

1. Reduction of heat losses with rear-ventilated façades

The construction of the rear-ventilated façades (RVF) from the main components of façade cladding, rear ventilation, insulation and substructure offers numerous advantages. In addition to the possibility of orderly dismantling at the end of the service life, there is a structural separation of weather and heat protection. Weather protection is ensured by the cladding elements. The air layer between the insulation layer and the cladding takes on a moisture-regulating function. [FVHF, 2017]. A common variant of the substructure is the combination of supporting profiles and brackets for load transfer within the façade system and the connection to the outer wall. The brackets penetrate the insulation level and thus represent punctiform thermal bridges. [Schild, 2018]. In addition to the number of brackets used, the size of the heat loss is determined by their material and geometry. To compensate for the losses, there is an option to increase the thickness of the thermal insulation. However, this approach is financially and ecologically unfavorable. The research project is therefore investigating the effect of using bath galvanized steel. The thermal conductivity of steel is well below the characteristic value of comparable materials such as aluminum, while at the same time the material is very rigid.

2. Façade cladding made of bath galvanized steel

Bath galvanized steel is being used more and more often as a material for façade cladding compared to the substructure. Occasionally, the substructure is made of bath galvanized steel, but these are individual solutions tailored to the project. The material is valued for its robustness and at the same time its appealing, lively zinc surface. Façade elements made of galvanized steel are preferred because they require almost no maintenance and can be completely recycled. The campus for the Zeppelin University in Friedrichshafen was completed on the former military site in Fallenbrunn in 2018 and received the Steel Innovation Prize 2018. The architects from as if designed the building shell as a RVF with 3 mm thick bath galvanized cladding elements (figure Figure 1). These are arranged in a grid of 3.00 x 1.60 m by means of concealed rear attachment to supporting profiles, which are also bath galvanized. In addition, the substructure is coated with a duplex system. The rounded corners of the building could also be made from bath galvanized sheet metal elements and fit exactly into the joint pattern. The window elements are adapted to the joint pattern and the rounded corners, resulting in a homogeneous, coordinated façade image [Stahl-Innovationspreis 2018] [Zinkpower 2022].

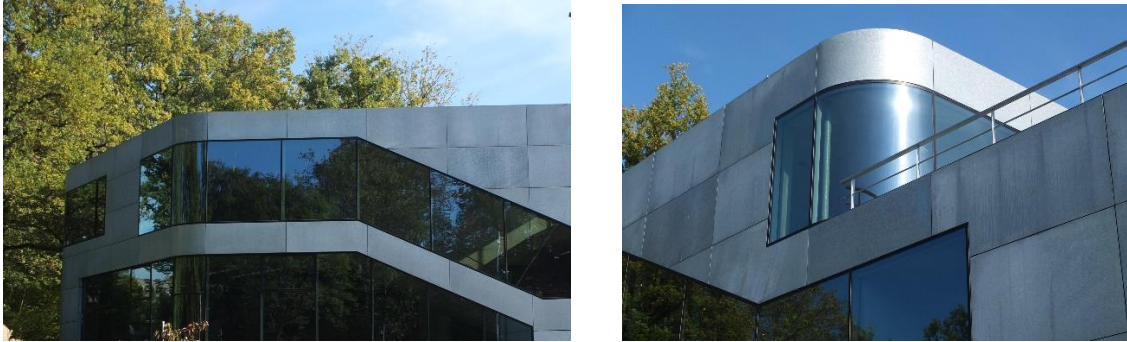


Figure 1: Zepplin University of Friedrichshafen, bath galvanized façade cladding, planning year 2012-13.

3. Designed bracket made of bath galvanized steel with low thermal bridge effect

The use of bath galvanized steel for the substructure creates opportunities to reduce heat loss through the façade. The low thermal conductivity of steel is one of the positive properties and achieves lower heat losses in the RVF-system. Due to the high material rigidity, the bracket distances can be increased, which reduces the number of localized thermal bridges. Simple L- and U-profile shapes are redesigned to minimize heat loss and at the same time have to ensure sufficient static properties for load transfer. Within the research project, four different brackets made of bath galvanized steel are being developed and examined. The reference bracket shown in figure 1 - variant 0 - is used for comparison. The focus of the design is on material efficiency. Perforations in the bracket sword reduce the heat-transferring surface and the contact area with the thermal insulation. Decisive for the reduction of heat losses is not only the largest possible perforation, but also a small cross-sectional area of the bracket sword. The cross-sectional area defines an assumed vertical section through the bracket blade. Steel also allows the use of thinner sheet thicknesses. This also affects the cross-sectional area. However, the perforations weaken the load-bearing capacity. This can be counteracted with flanges in the edge areas of the perforations and edging on the upper and lower edges. These increase the rigidity of the free edges of the sheet and increase resistance to buckling [Klein, 2018].

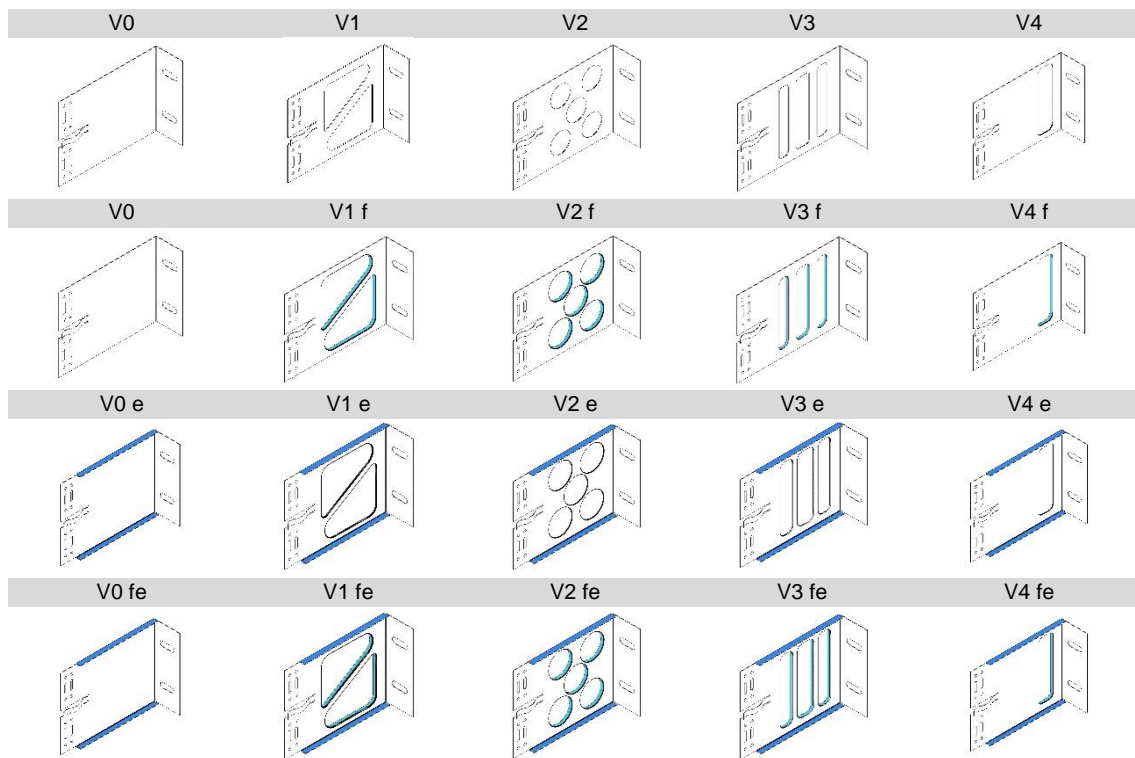


Figure 2: Four bracket variants with different hole geometries f: with flanging, e: with edges, fe: with flanging + edges.

4. Substructure suitable for galvanizing

The supporting profiles and brackets were manufactured in the metal workshop of the Dortmund University of Applied Sciences and Arts for galvanizing, and the piece galvanizing was carried out in the Coatinc Company Holding galvanizing plant in Bochum. For the galvanizing process, the small-format L-angles were fixed to the long holes of the bracket on the wall using the common method of wire suspension on the traverse (

Figure 3). This resulted in smaller accumulations of zinc or zinc detachment due to stripping (**Figure 4** and Figure 5). These changes also occurred in the second series of tests, in which the galvanizing time was increased to 12 minutes and the loops of the wire suspension were enlarged. However, these are minimal in relation to the size of the component. The largest areas are approx. 12 mm x 4.1 mm and are below the prescribed area of [EN ISO 1461, 2009]. The area should not exceed 0.5 % of the total surface area of the component and should not be larger than 10 cm². A touch-up with zinc dust paint is permissible with these dimensions and should result in a layer thickness of 100 µm and also cover the edge areas (Figure 5, right). Perforations were made for the suspension for the supporting profiles, since no perforations are planned in the design. No surface changes can be seen on the supporting profiles.



Figure 3: Enlarged loop formation of the wire suspension (left); Extraction process of the galvanized components (right).



Figure 4: Zinc accumulation at the elongated hole due to the wire suspension (left) Detachment of the zinc layer due to dismantling (right).

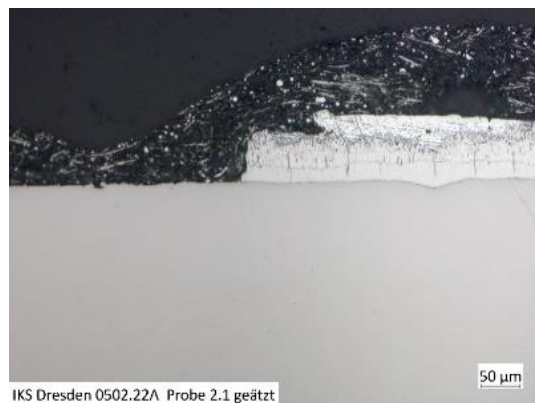
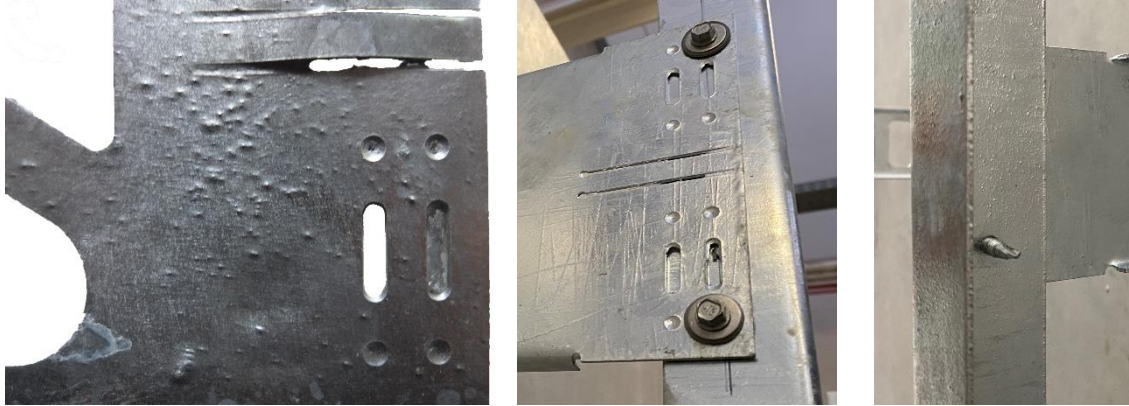


Figure 5: Micrographs: Missing zinc coating due to wire imprint (left); Touch-up with zinc dust paint. The edges are covered as required (right) [IKS Dresden].

Holes are provided at the top of the bracket sword for fixing between the bracket and the supporting profiles. The diameter of the round hole is 5 mm and the width and length of the elongated hole is 5 mm x 20 mm. Figures 6 shows that the round holes are sealed with zinc after galvanizing and zinc spangles have formed in the round holes. A larger perforation is not possible, as the diameter of common self-drilling screws must be taken into account. It has been proven that self-drilling screws can be inserted into the component with closed holes (Figures 6, middle

and right). The zinc coating is positive for assembly. When fixing the support profile to the bracket using self-drilling screws, the zinc will remain in the perforations and serve as additional protection against corrosion. To avoid these hole closures, it is possible to centrifuge the brackets after the piece galvanizing. This was not investigated further in this work.



Figures 6: Closing the round holes with zinc and formation of zinc flakes in the oblong holes (left) Use of self-drilling screws to mount the supporting profiles on the bracket (middle and right).

The suitability for batch galvanizing was checked on both types of components in terms of angularity and sufficient formation of the zinc layer in accordance with [EN ISO 1461, 2009]. It was to be assumed that the components made of thin sheet metal would warp or that the zinc layer would not be sufficiently thick. The following sheet thicknesses 0.8 mm; 1.0 mm; 1.5 mm; 2.0 mm were examined. In addition, there are investigations on two meter long support profiles. Based on measurements before and after galvanizing, the statement can be made that there were no distortions in the thin and long substructure components. Additional documentation of the components was carried out using a series of photos. Figure 7 Figure 8 show an excerpt. The layer thicknesses were determined using a magneto-inductive method. The averaged values in Table 1 and Table 2 show the average zinc layer thickness of the components. The values are compared with the specifications of [EN ISO 1461, 2009]. All values are above the required minimum values from the standard.

Table 1: Results of the average layer thicknesses - brackets. Mean values of all average layer thicknesses of variants 0 to 4 according to sheet thickness.

brackets				
sheet thickness	minimum value DIN 1461	Measured average layer thickness with different galvanizing times		
		test series 1	test series 2	
		9 min.	9 min.	12 min.
[mm]	[μm]	[μm]	[μm]	[μm]
0.80	45	62.6	76.2	85.5
1.00	45	64.7	77.0	87.5
1.50	55	57.7	78.7	84.1
2.00	55	59.3	84.5	84.9
2.50	55	62.0	k. A.	k. A.
3.00	55	65.3	k. A.	k. A.

Table 2: Results of the average layer thicknesses - supporting profiles. Mean values of all average layer thicknesses of the variants according to sheet thickness.

supporting profiles				
sheet thickness	minimum value DIN 1461	Measured average layer thickness with different galvanizing times		
		test series 1	test series 2	
		9 min.	9 min.	12 min.
[mm]	[μm]	[μm]	[μm]	[μm]
0,80	45	58.3	78.1	81.1
1,50	55	72.9	74.7	79.8
2,50	55	70.6	86.9	90.6



Figure 7: Excerpt of photo documentation: wall bracket variant 0; test series 1; t=1.00mm, steel 235, before galvanizing (left) after galvanizing (right).

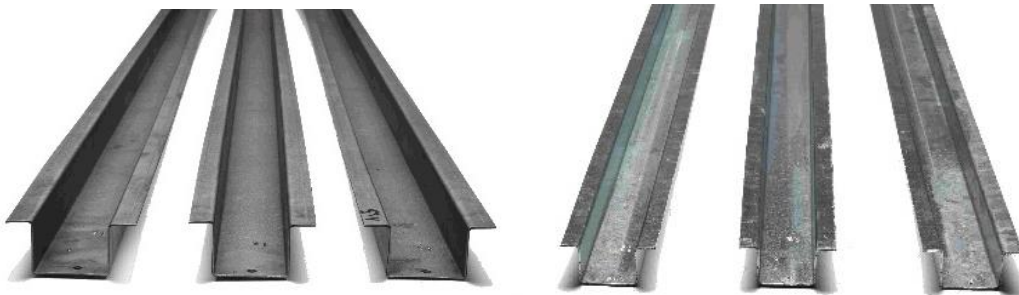


Figure 8: Excerpt of photo documentation: hat-supporting profile, test series 1; t= 1.50 mm; Steel 235 before galvanizing (left) after galvanizing (right).

5. Mechanical investigations

In the research project, the load-bearing capacity and the load-deformation behavior of the designed brackets and supporting profiles were examined using a testing machine. The examinations of the brackets are based on German standard [DIN 18516-1, 2010] and are tested under pressure and 45° diagonal tensile stress. The 3-point bending test carried out in the project is based on [EN ISO 7438, 2021] for stressing the supporting profiles. The diagram in Figure 9 is an excerpt from the tests and shows the stress on the bracket (variant 3) with edge edging and flanging under 45° diagonal tensile stress. This load corresponds to an interaction between dead load and wind suction. With a deformation of 3 mm, the bracket was loaded with a force of 612 N and with a deformation of 10 mm with 1,965 N. In summary, the 45° diagonal pull test shows that the brackets fail due to the load on the wall-side flange (Figure 10, right). The plasticization

decreases with increasing sheet thickness. The stability is increased by the introduction of the flanging and the edge folds result in a further and higher increase in the absorption of the loads. At the end of the project, the results will be compared with those from the numerical simulations.

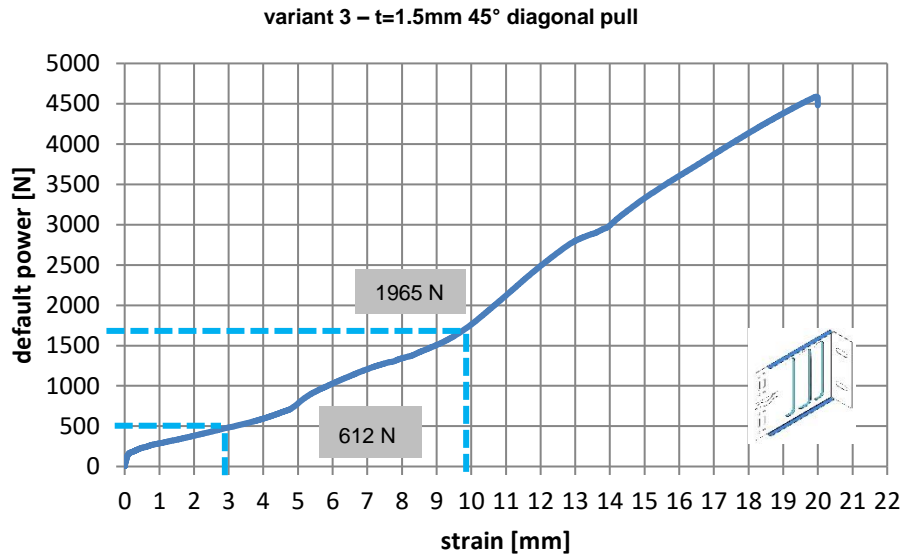


Figure 9: Diagram of a bracket variant 3, t=1.5 mm, with flanges and edges under 45° diagonal tensile stress.

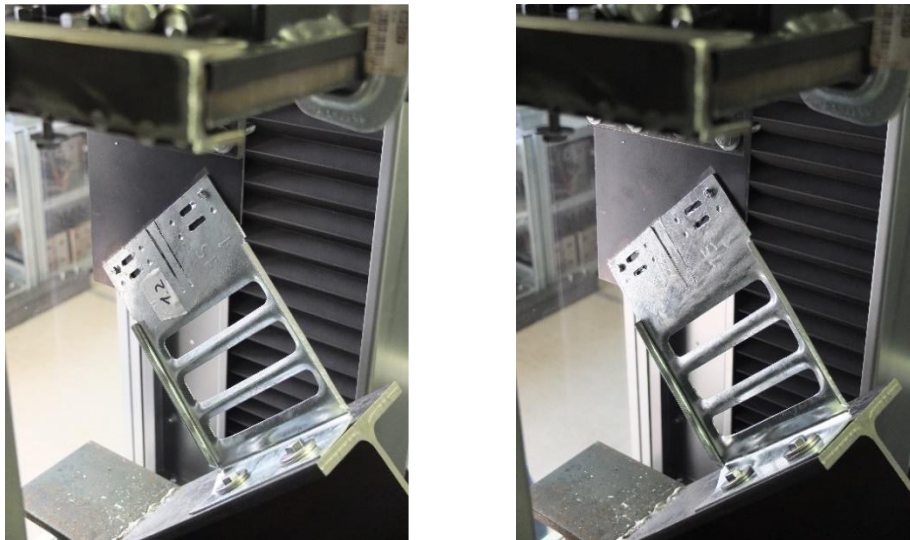


Figure 10: Structure of the 45° diagonal pull test in the testing machine with built-in wall bracket before (left) and after (right) the loading.

6. Numerical analysis of the mechanical and thermal properties

As a component of the building envelope, the rear ventilated façade is exposed to numerous environmental influences and impacts. In addition to moisture that precipitation can bring into interspace of façade, it also brings in corrosive pollutants. Temperature effects, which can be assumed to be in a range between -20 °C and +80 °C, cause materials to expand. In practice,

constructive measures have proven successful largely exclude damage to façade by these effects. For example, constraint stresses on façade components are avoided by forming sliding bearings in form of elongated holes. The design relevant loads on façade are divided into permanent and variable loads. Permanent loads include dead-load of façade as a vertical load, which is largely determined by the type and material of cladding elements. In addition, the weight of heavy cladding elements is increased by a stronger dimensioning of substructure. Snow and ice loads represent variable actions, but their effect depends on surface properties of cladding elements. For example agglomeration of snow is possible with a façade greening. Wind suction and wind pressure loads act as horizontal variable effects on façade.

The mechanical analysis of brackets as a function of decisive actions is carried out on a numerical model using finite element method. Under compressive load brackets exhibit pronounced buckling behaviour. In load-deformation curve, load increases proportionally with deformation until no further increase of loads is possible with increasing deformation. Especially brackets with perforations are susceptible to buckling. The added flanges and bendings of brackets stabilise them in corresponding areas. For loading of brackets under tension and dead load, test setups were modelled according to [EAD 090034-00-0404, 2017]. Under vertical load, compressive forces occur in lower area of brackets; bends also have a positive effect on load. Under tensile load, strongest deformations occur in the area of 90° angle on wall side of brackets. The structure lifts off the wall around anchoring means.

The determination of a favourable bracket geometry that optimally combines mechanical and thermal properties additionally requires an evaluation of the thermal properties of brackets. Following [EN ISO 10211, 2018], the model for thermal analysis is defined as a square wall section with the surface of 1 m². The profiles are not taken into account in the thermal evaluation of bracket shape, in accordance with assumption of a strongly ventilated air layer according to [EN ISO 10211, 2018].

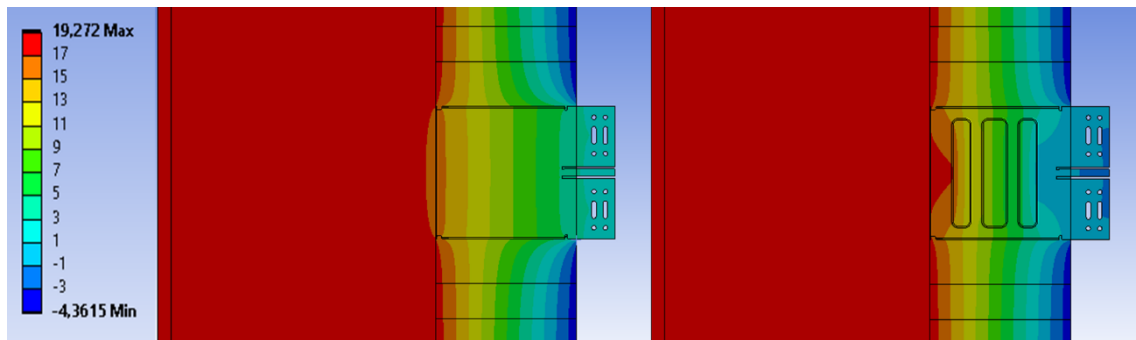


Figure 11: heat flow, left: bracket variant V0 fe, right: variant V3 fe with rectangular perforations

As a result, the lowest surface temperature on inner wall surface and the thermal bridge coefficient are evaluated and compared. The smallest improvement in both results is achieved by bracket types of variant 2 compared to the reference bracket 0. Offset circular perforations reduce heat conduction, but the large continuous webs between the recesses have an unfavourable effect. For variant 4, the temperature on inner wall surface is slightly higher. The opening that extends over the entire height of the bracket has a positive effect. Since this only fills a small area in the rear part of bracket, point thermal transmittance is not lowered to the same extent as with variant 3. With bracket types of variant 1, point thermal transmittance is further reduced, but the diagonal in the large rectangular opening increases thermal conduction. Variant 3, shown in Figure 11 as V3 fe on the right, provides most favourable results with the lowest value and the highest

temperature on the inner wall surface. Compared to variant 4, the rectangular openings are arranged over the entire bracket projection.

For a combined assessment of mechanical and thermal quality of brackets, a façade section of 3 m height and 1 m width is examined. Under specified horizontal and vertical loads, the required number of brackets for the façade section is determined using the values calculated for load-bearing capacity of brackets. The initial value is the thermal transmittance of the thermally undisturbed wall. With the thermal bridge coefficient of individual bracket variants from thermal investigation, thermal transmittance can be corrected according to the number of brackets. A lower thermal transmittance of façade section with bracket variant stands for a favourable influence on the heat losses.

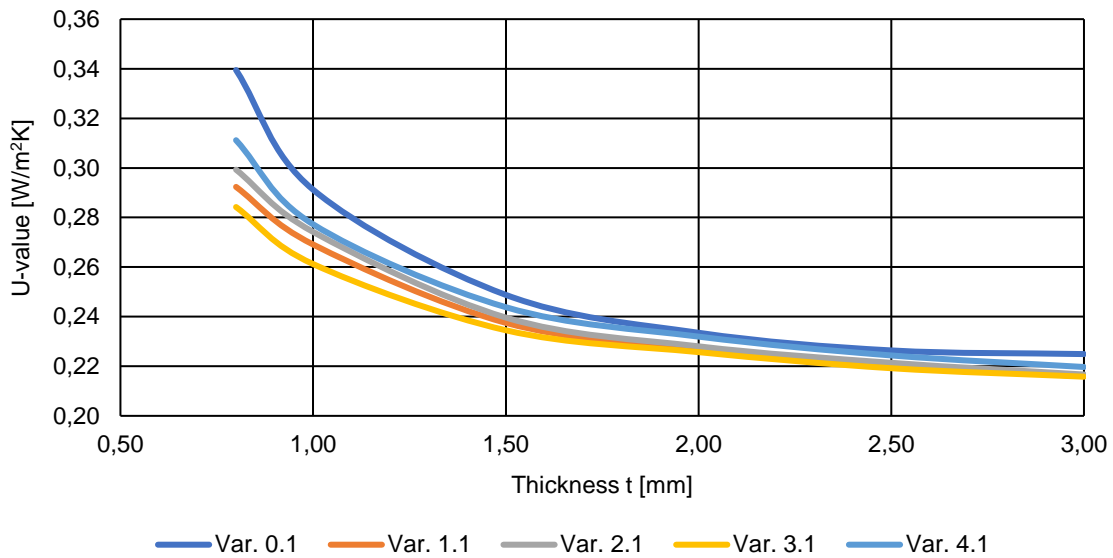


Figure 12: Thermal transmittance for a wall section with different bracket variants in various sheet thicknesses

The diagram shows an example of thermal transmittance of the façade section for bracket variants without bendings and flanges. The positive effect of the perforations in brackets can be seen especially with the low sheet thicknesses. Variant 3 and 1 achieve the lowest U-value. With increasing sheet thickness, the influence of perforations is reduced, as the number of individual brackets required also decreases. Overall, it has a more favourable effect on heat losses to use a smaller number of more strongly dimensioned brackets with a higher thermal bridge coefficient than a large number of less strongly dimensioned brackets with a low thermal bridge coefficient.

7. Literature

Ansys Inc.(2020), Ansys Workbench Release 2, CADFEM GmbH, München.

DIN 18516-1:2010. Cladding for external walls, ventilated at rear Part 1: Requirements, principles of testing, Berlin: Beuth, 2010.

EAD 090034-00-0404: 2017: Kit composed by subframe and fixings for fastening cladding and external wall elements, European Assessment Document. Brussels: EOTA, 2016

EN ISO 10211:2018. Thermal bridges in building construction Heat flows and surface temperatures, Detailed calculations. Berlin: Beuth, 2018.

EN ISO 1461:2009. Hot dip galvanized coatings on fabricated iron and steel articles Specifications and test methods. Berlin: Beuth, 2009.

EN ISO 7438:2021. Metallic materials – Bend test. Berlin: Beuth, 2021.

EN ISO 6946:2018. Building components and building elements - Thermal resistance and thermal transmittance - Calculation methods. Berlin: Beuth, 2018,
FVHF (2017). Planung und Ausführung - FVHF-Leitlinien. Berlin.

Klein, B. und Gänsicke, T. (2018), Leichtbau-Konstruktionen – Dimensionierung, Strukturen, Werkstoffe und Gestaltung. Wiesbaden: Springer.

Schild, K. (2018), Wärmebrücken – Berechnung und Mindestwärmeschutz. Wiesbaden: Springer Vieweg.

Stahl-Innovationspreis (2018), http://www.stahl-innovationspreis.de/wp-content/uploads/2018/06/D503_Stahl_Innovationspreis_2018-1.pdf. 09.06.2022.

Zinkpower (2022) <https://www.zinkpower.com/media/files/mediaspiegel/zp-feuerverzinkte-fassade-bibaum.pdf>. 09.06.2022.

8. Figure source

IKS - Institut für Korrosionsschutz Dresden GmbH, Sixx, S.; Thorke, R.: Werkstoffanalyse vom 22.02.2022.